Eutectic cleavage of lignocellulosic biomass to incubate pseudo-graphitic carbon crystallites for high-efficiency sodium energy

Fengxuan Wu [a, #], Yueying Li [b, #], Mingyao Wang [a], Weijia He [a], Mingwei Jiang [a], Dan Su [a], Jiaping Zhang [a], and Jian-Gan Wang [a, b, *]

[a] *State Key Laboratory of Solidification Processing, Center for Nano Energy Materials School of Materials Science and Engineering, Northwestern Polytechnical University and Shaanxi Joint Lab of Graphene (NPU), No. 127, Youyi West Road, Xi'an 710072, China*

[b] *School of Energy and Electrical Engineering, Qinghai University, Xining 810016, China*

The authors contribute equally to this work.

E-mail addresses: wangjiangan@nwpu.edu.cn (J.-G. Wang).

Experimental

Materials synthesis

The ChCl/urea deep eutectic solvent (DES) was first synthesized by mixing choline

chloride and urea in a 1:2 molar ratio, followed by stirring at 80 °C for 2 h until a transparent homogeneous liquid formed. Subsequently, 3 g of dried walnut shell power was treated with 100 mL of the as-prepared DES at 120 °C for 6 h under constant stirring. After the mixture cooled naturally to ambient temperature, the solid residue, denoted as DES-treated walnut shell (DES-WS), was collected by filtration and thoroughly dried at 60 °C. The final hard carbon material (marked as DES-HC) was obtained by pyrolyzing the DES-WS precursor at 1300 °C for 2 h under a continuous argon flow. For comparison, a pristine hard carbon sample (P-HC) was prepared directly from the walnut shell powder (WS) using an identical pyrolysis procedure, but omitting DES treatment step. The carbon yield of DES-HC was decreased slightly from 23.1% to 19.8% due to the removal of some hemicellulose and lignin during DES treatment.

Materials characterization

Functional groups were identified by Fourier transform infrared (FTIR) spectroscopy (Nicolet-iS50). The crystalline structures and defect features were examined by X-ray diffraction (XRD, X'Pert PRO MPD) using Cu-Kα radiation (λ=1.54056 Å) and by Raman spectroscopy (Renishaw in Via RM2000) with a 532 nm excitation laser. The detailed morphologies were observed by scanning electron microscopy (SEM, FEI NanoSEM450) and high-resolution transmission electron microscopy (HRTEM, Talos F200X). The elemental compositions were analyzed by X-ray photoelectron spectroscopy (XPS) on a Shimadzu Kratos Axis Supra system. The specific surface area and pore size distributions were derived from N_2 adsorption-desorption isotherm analysis, while the closed porosity was evaluated through small-angle X-ray scattering (SAXS, Xeuss 2.0). The true density testing was determined on a helium pycnometer (Ultrapyc 3000). UV-vis absorption spectra were recorded on a Lambda 35 spectrophotometer (PerkinElmer).

Electrochemical measurements

HCs anodes were prepared by casting a slurry of HCs, carboxymethyl cellulose and Super P (mass ratio= 8:1:1) in deionized water onto a Cu foil. The coated electrodes were vacuum-dried at 105 °C overnight and then punched into 12 mm diameter discs, with an

average active material mass loading of ~1.5 mg cm^{-2}. Coin cells (CR2032 type, Canrd Technology Co. Ltd) were assembled in an argon-filled glove box, using sodium metal (Changgao New Materials Co., Ltd) as counter/reference electrode, a Whatman GF/D glass microfiber separator, and an electrolyte of 1.0 M $NaPF_6$ in diglyme. The electrochemical workstation (CHI660D) was employed to collect the cyclic voltammetry (CV) curves at various scan rates and electrochemical impedance spectroscopy (EIS) over a frequency range of 10^5-0.1 Hz. Galvanostatic charging-discharging (GCD) technique was applied to assess the rate and cycling performances within a potential window of 0.01-2 V (vs Na/Na^+). Galvanostatic intermittent titration technique (GITT) adopted 0.5 h current pulse at 0.02 A g^{-1} followed by a 2 h relaxation interval. The full-cell was assembled by pairing a commercial sodium vanadium phosphate (NVP) cathode with the DES-HC anode with a negative/positive (N/P) capacity ratio of 1.1:1. To compensate for the irreversible Na^+ consumption induced by SEI formation, presodiation was performed on the HC anode prior to the full cell assembly. The electrochemical performance of the NVP||DES-HC full-cell was evaluated with a fixed voltage range of 1.5-3.8 V.

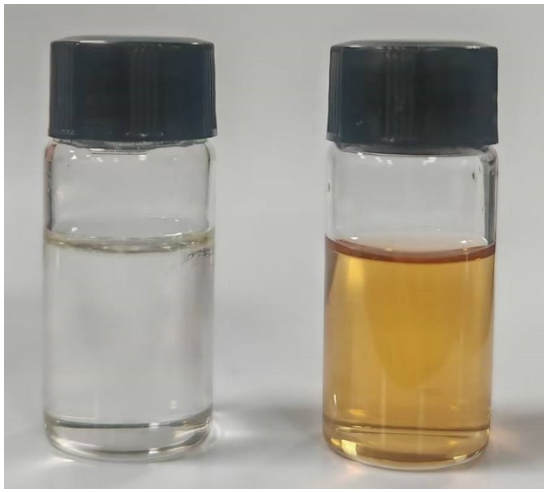

Figure S1 The digital images of DES solution before (left) and after (right) WS dipped.

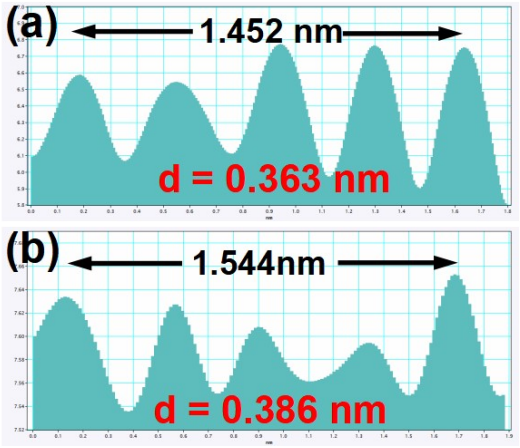

Figure S2 The measurement of interlayer spacing in different regions in HRTEM: (a) P-HC, and (b) DES-HC.

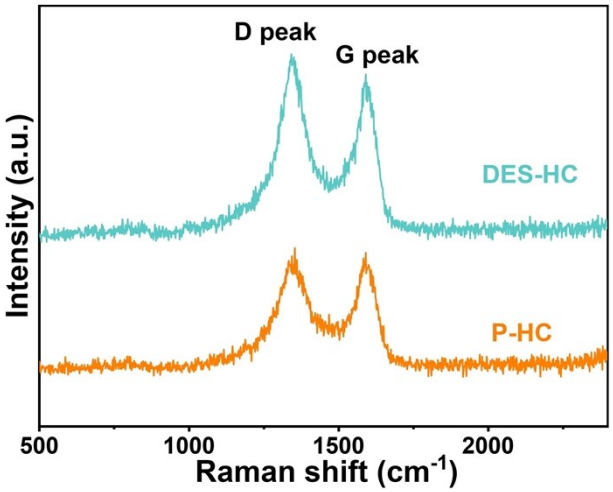

Figure S3 The Raman spectra of P-HC and DES-HC.

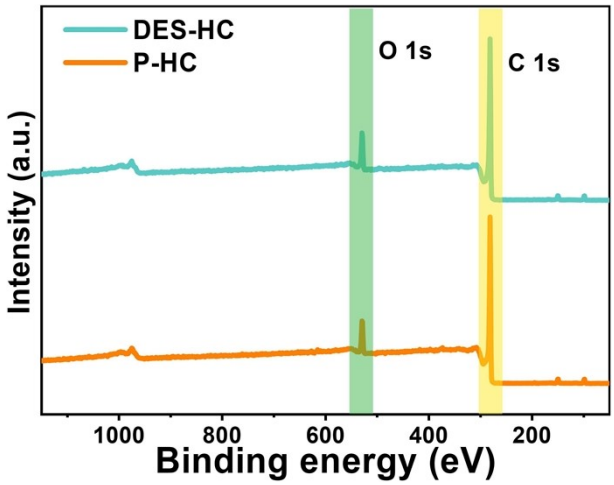

Figure S4 The XPS full spectra of P-HC and DES-HC.

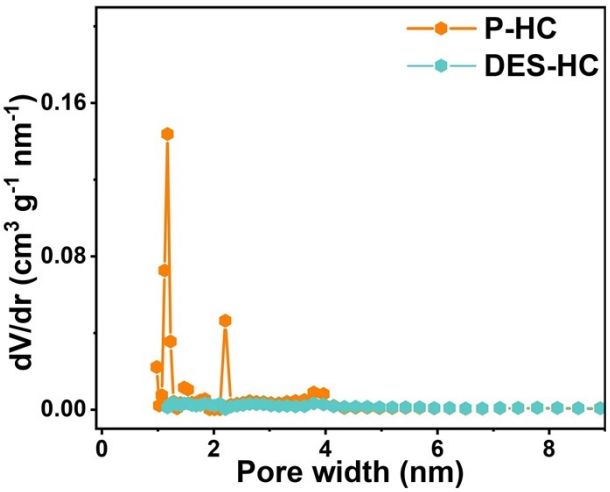

Figure S5 Pore size distribution of P-HC and DES-HC.

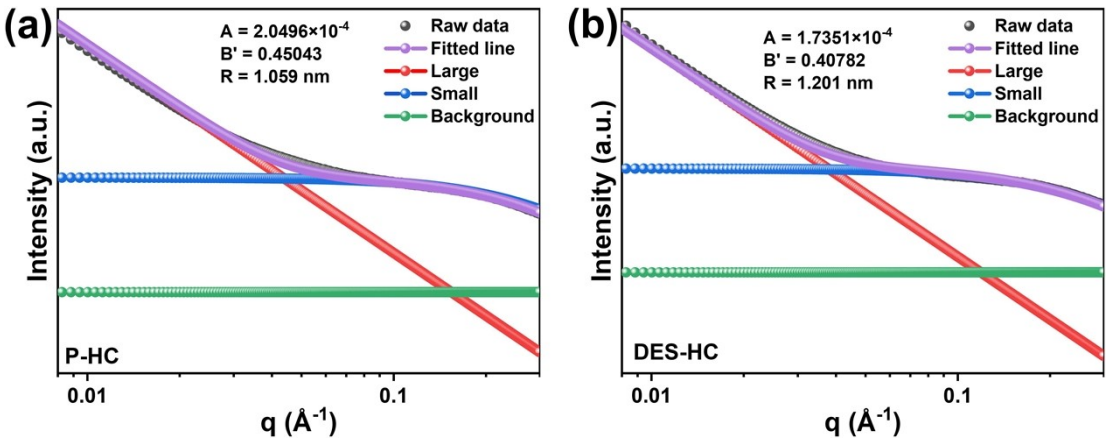

Figure S6 Fitted SAXS patterns of (a) P-HC, and (b) DES-HC.

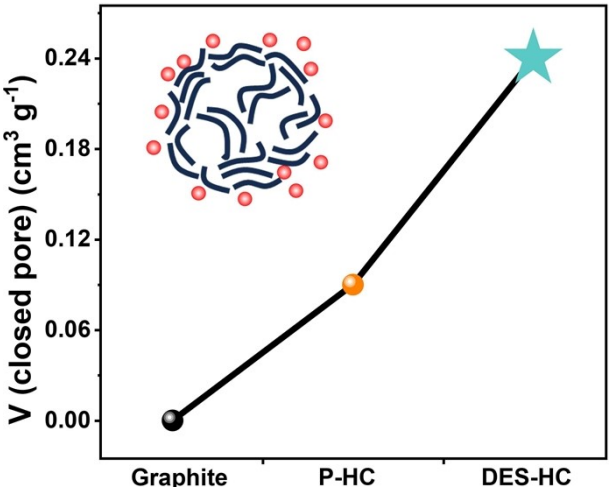

Figure S7 Comparison of closed-pore volume of DES-HC and P-HC

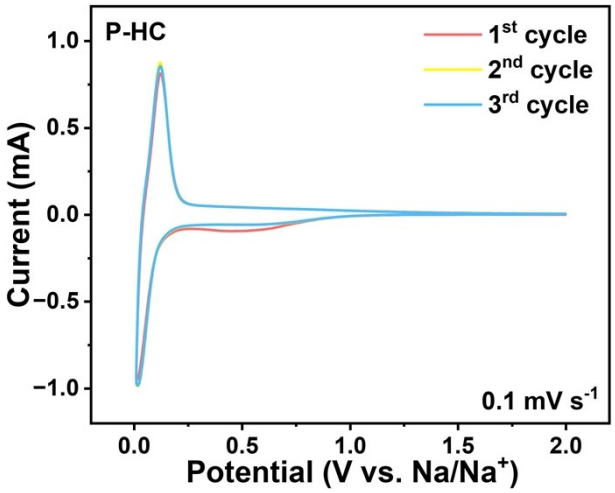

Figure S8 The first three CV curves of P-HC.

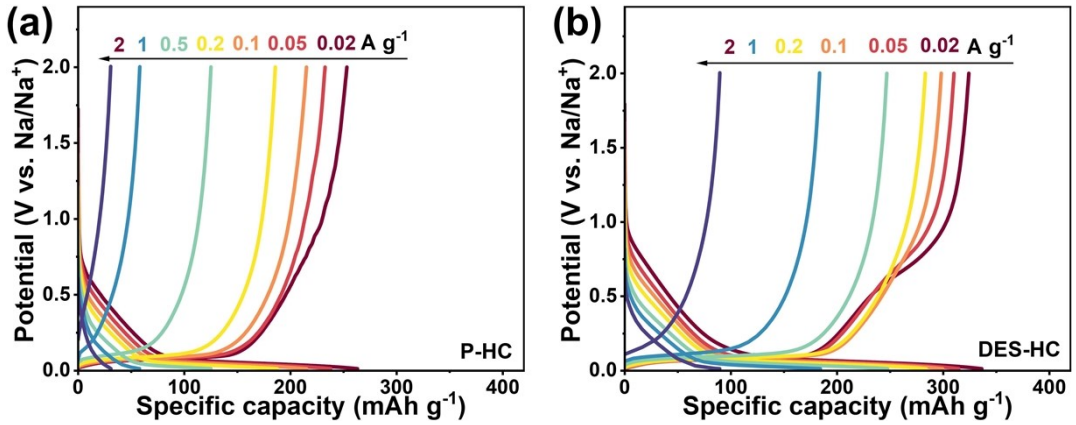

Figure S9 GCD curves of (a) P-HC, and (b) DES-HC at different scan rates.

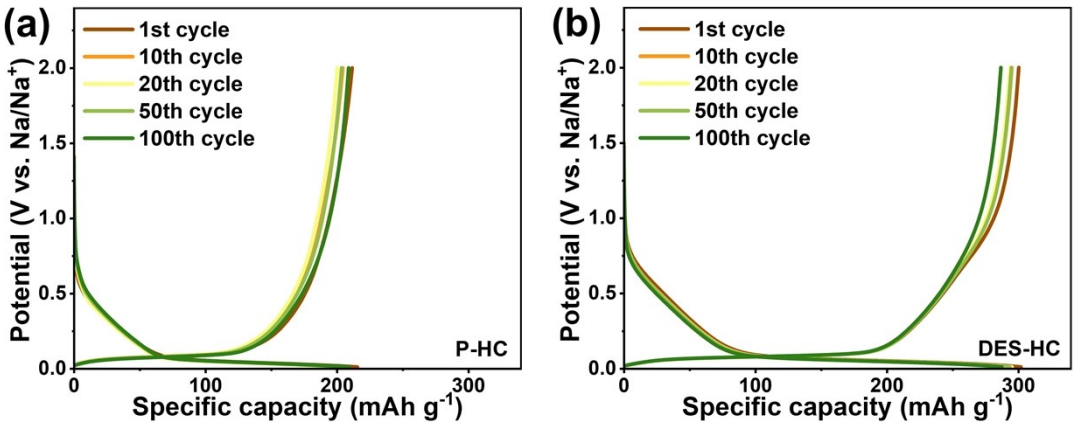

Figure S10 GCD curves of (a) P-HC, and (b) DES-HC at 0.1 A g^{-1}.

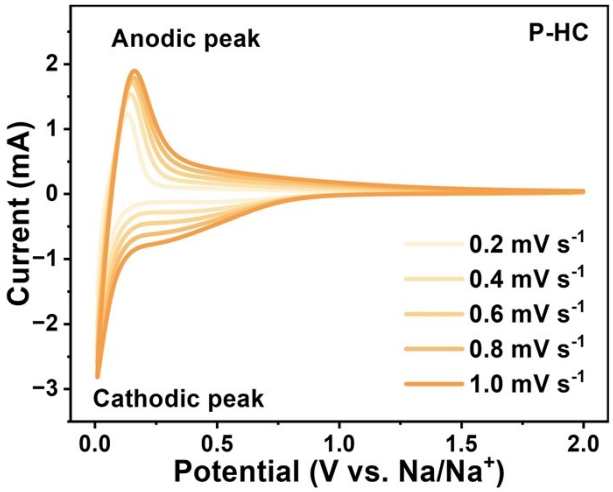

Figure S11 CV curves of P-HC under different scan rates.

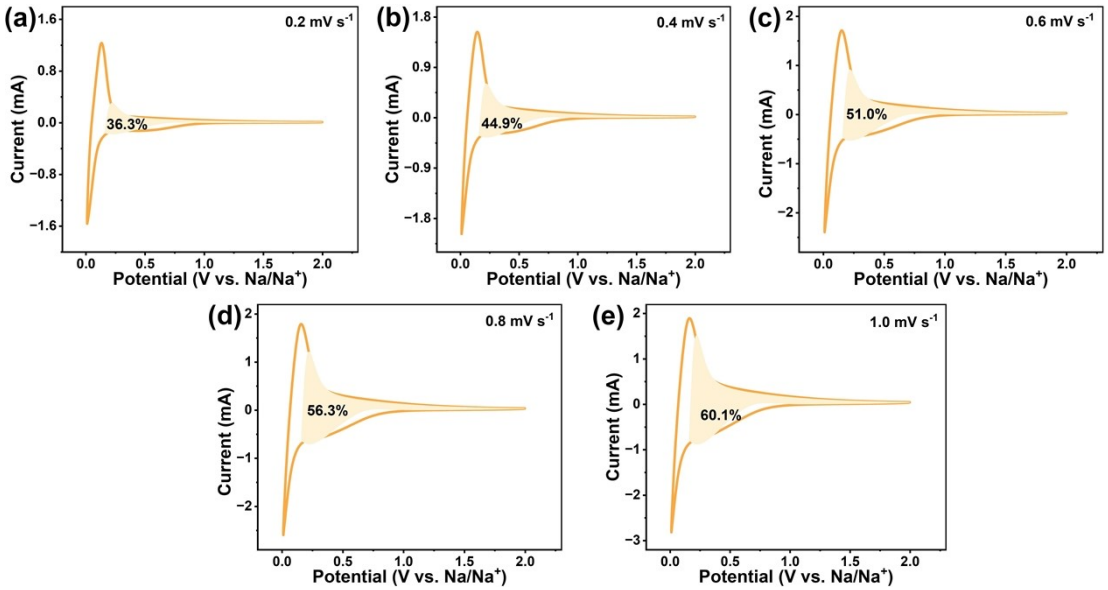

Figure S12 The capacitive contribution of P-HC electroe at (a) 0.2, (b) 0.4, (c) 0.6, (d) 0.8 mV s^{-1}, and (d) 1 mV s^{-1}.

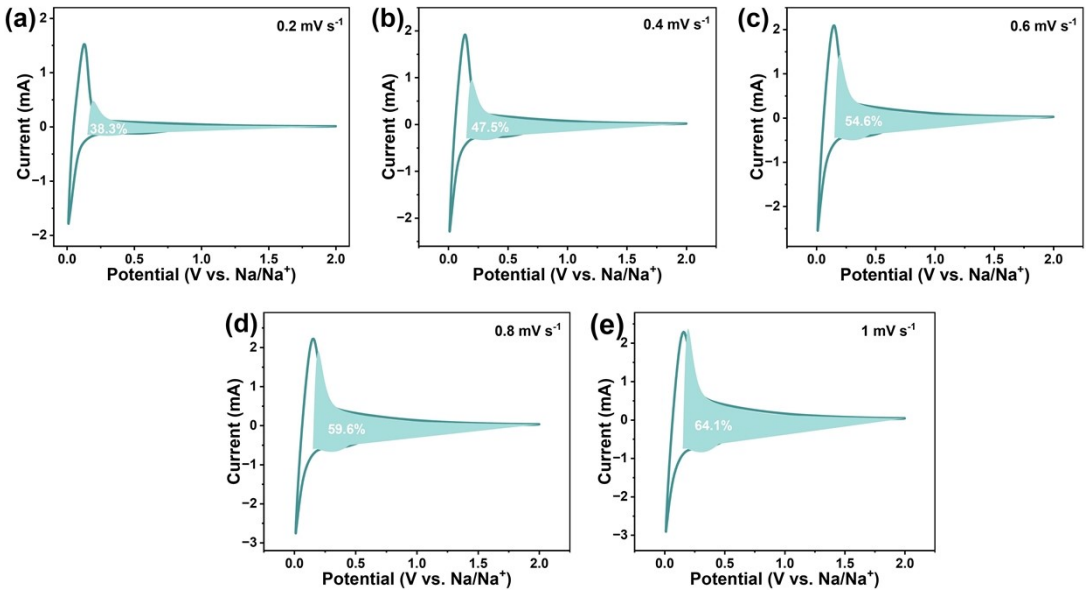

Figure S13 The capacitive contribution of DES-HC electroe at (a) 0.2, (b) 0.4, (c) 0.6, 0.8 mV s^{-1}, and (d) 1 mV s^{-1}.

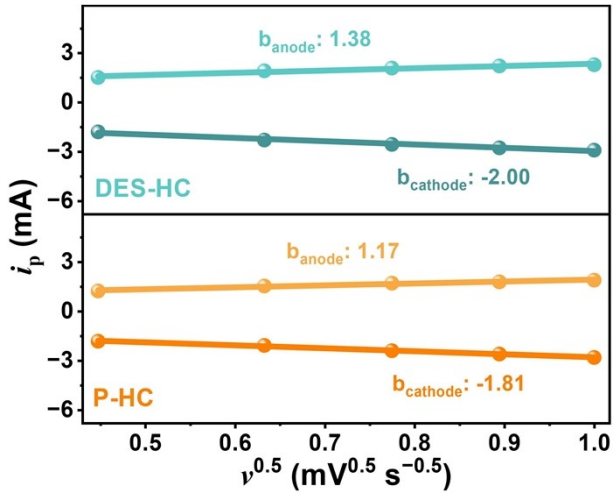

Figure S14 Fitting of the b values of the cathode and anode peaks

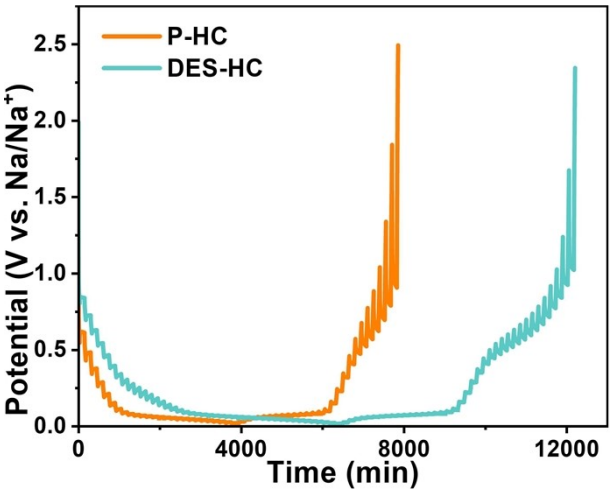

Figure S15 GITT curves at 0.02 A g^{-1}

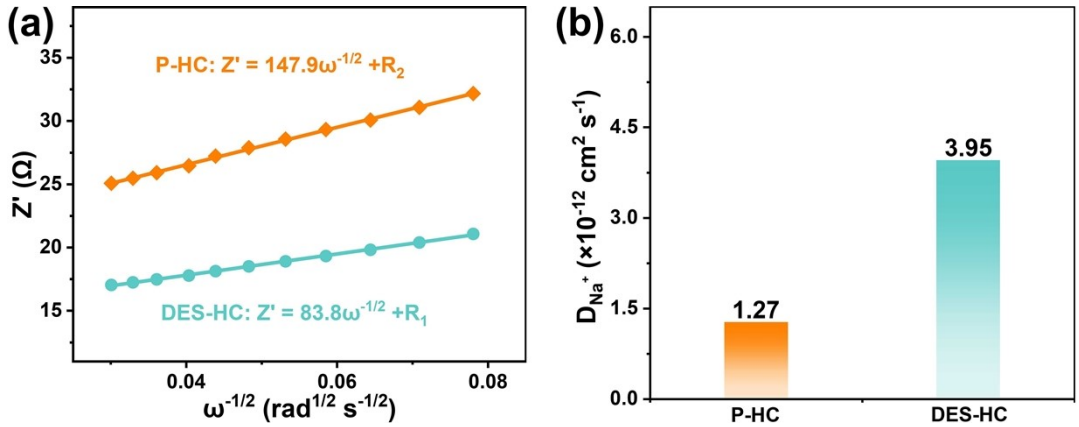

Figure S16 (a) The linear fitting of Z' and $\omega^{-1/2}$ and (b) the corresponding Na^+ diffusion coefficients.

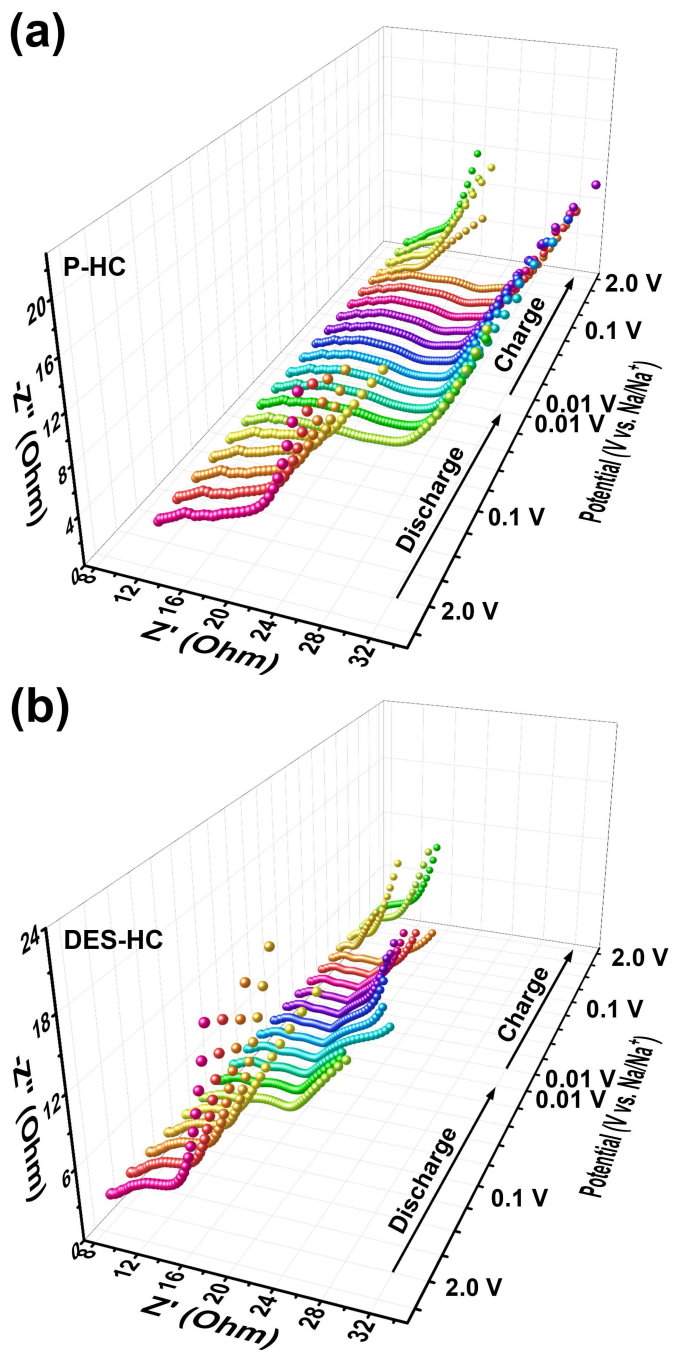

Figure S17 *In-situ* EIS test: (a) P-HC, and (b) DES-HC.

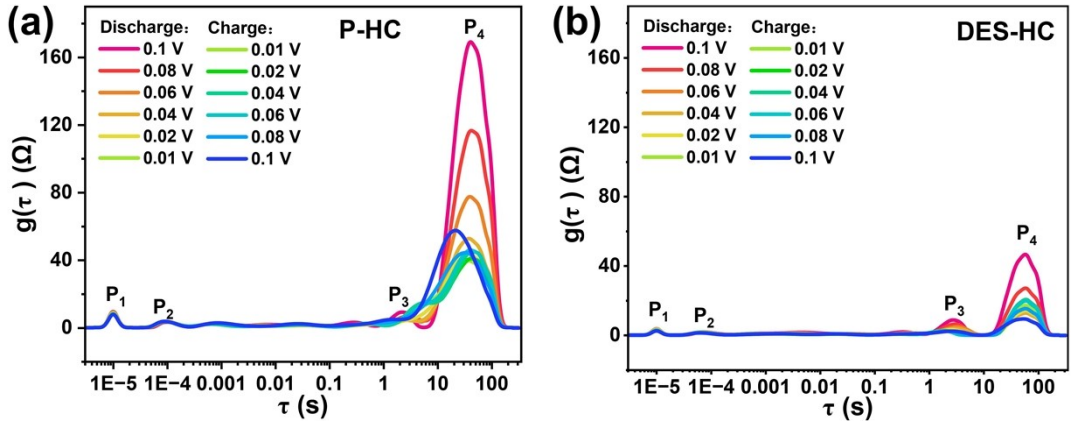

Figure S18 Time relaxation characteristic peaks of (a) P-HC, and (b) DES-HC electrodes

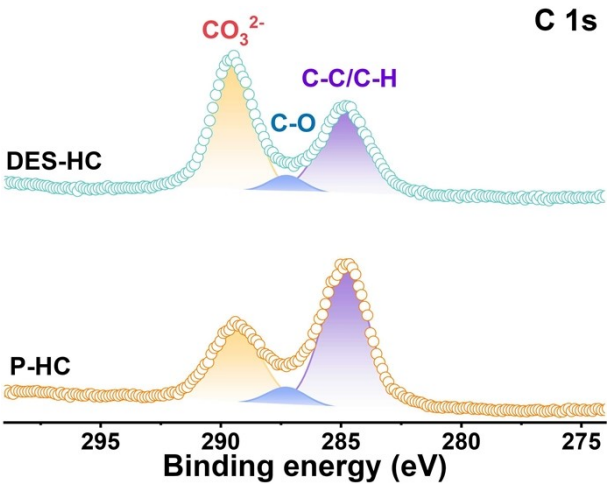

Figure S19 High resolution XPS spectra of C 1s in cycled P-HC and DES-HC.

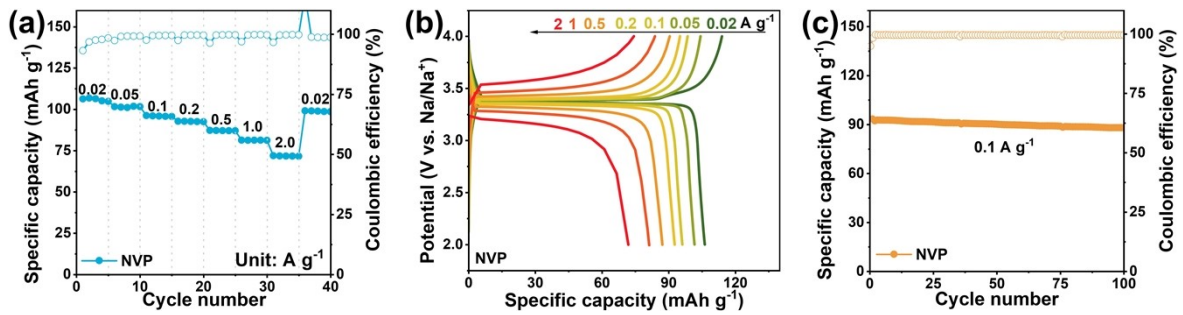

Figure S20 The electrochemical performance of NVP cathode: (a) rate property, (b) GCD curves, and (c) Cycling stability.

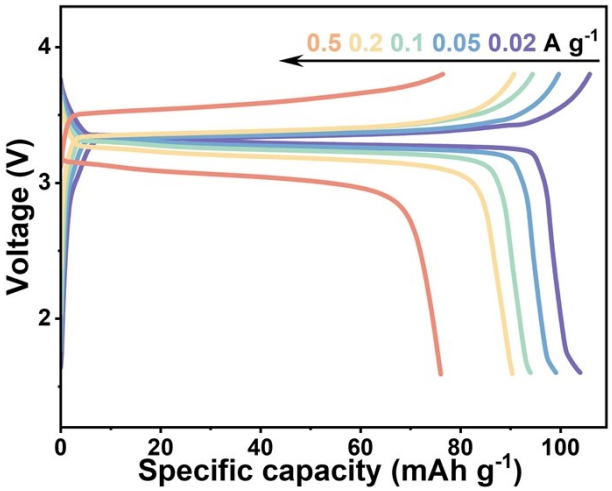

Figure S21 GCD curves of full cell at different current densities.